Electronic Supplementary Material (ESI) for Polymer Chemistry.
This journal is © The Royal Society of Chemistry 2015

Electronic Supplementary Information

Unraveling the Forming Mechanism of Hierarchical Helices via Self-assembly of an Achiral Supramolecular Polymer Brush

Shanshan Liu, Qibin Chen*, Yujie Sheng, Jincheng Shen, Changjun Peng, Honglai Liu*

State Key Laboratory of Chemical Engineering, East China University of Science and Technology, 130 Meillong Road, Shanghai 200237, China. Fax: +86 21 6425 29211; Tel: +86 21 6425 2921. E-mail: qinbinchen@ ecust.edu.cn; hlliu@ecust.edu.cn.

Characterization Data

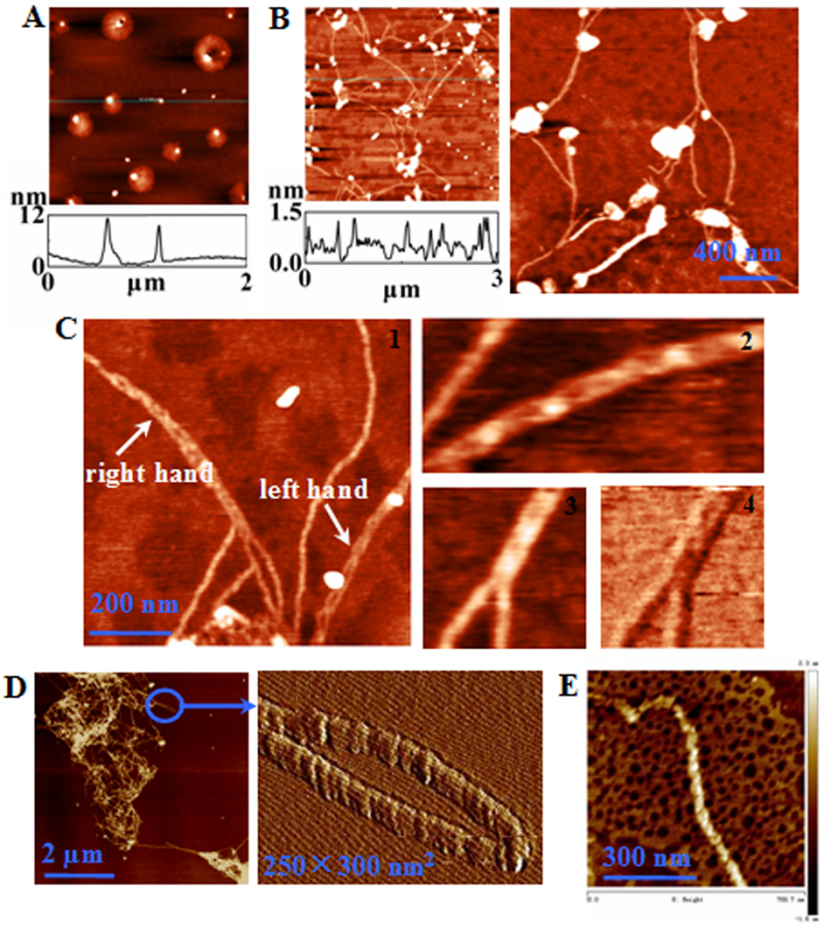

Fig. S1. The AFM images of the spin-coating film of PVP-PDP at 5.0×10^{-4} mol·L^{-1} (A), LB films of PVP-PDP at different surface pressures, 2 mN/m (B), 5 mN/m (C), 15 mN/m (D) and 25 mN/m (E). In B, the size of panels 2 and 3 is 345 × 157 and 180 × 180 nm^2, respectively, and panel 4 is the phase image of panel 3. In C, the local amplified image is phase image.

At 2 mN/m, one can clearly observe two and three fibrils can twist and form nanofibers

with a double helix and a triple helix (Fig. S1B). In Fig. S1C, the panel 1 shows a right-handed quadruple helix and a left-handed double helix. Moreover, the double helix in panel 2 presents a right-handed conformation, while that in panel 2 and 3 (Fig. S1C) shows a left-handed structure. The results suggest the handedness of such helices is formed by chance. At higher surface pressure (Fig. S1D and S1E), these nanofibers could further self-organize into larger aggregates. Herein, Fig. S1D and S1E were obtained from Bruker AXS Dimension Icon microscope in ScanAsyst-Air mode with a spring constant of 0.4 $N \cdot m^{-1}$ and a resonance frequency in the range of 50-90 kHz.

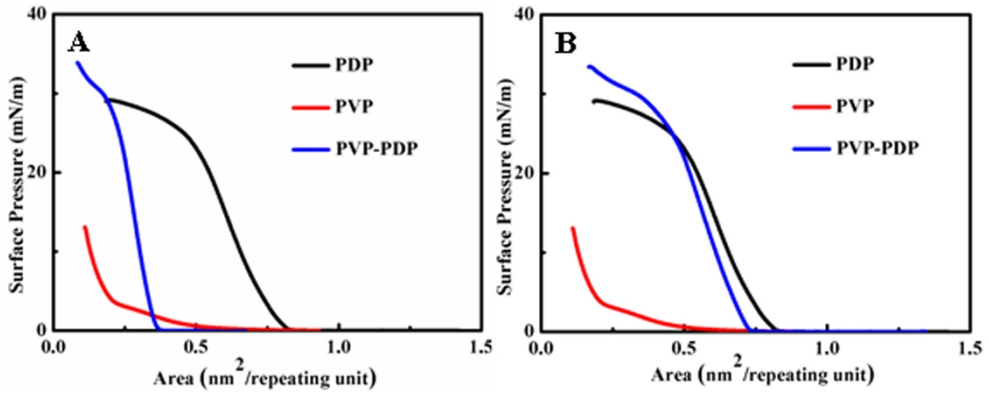

Fig. S2. π-A isotherms of PVP, PDP, and PVP-PDP at 5.0×10^{-4} $mol \cdot L^{-1}$.

In Fig. S2A, the molecular area of PVP-PDP was based on the average molecular weight of PVP and PDP, while in Fig. S2B, this value was only on the molecular weight of PDP. In Fig. S2, the liftoff areas of pure PVP (repeat unit) and PDP are 0.65 and 0.87 nm^2, while this area of PVP-PDP in Fig. S2A and B is 0.38 and 0.77 nm^2, respectively. The latter value indicates that the molecular area of PDP in complex film is less than that in the pure monolayer to some extent, suggesting that an intermolecular association does take place between PVP and PDP.

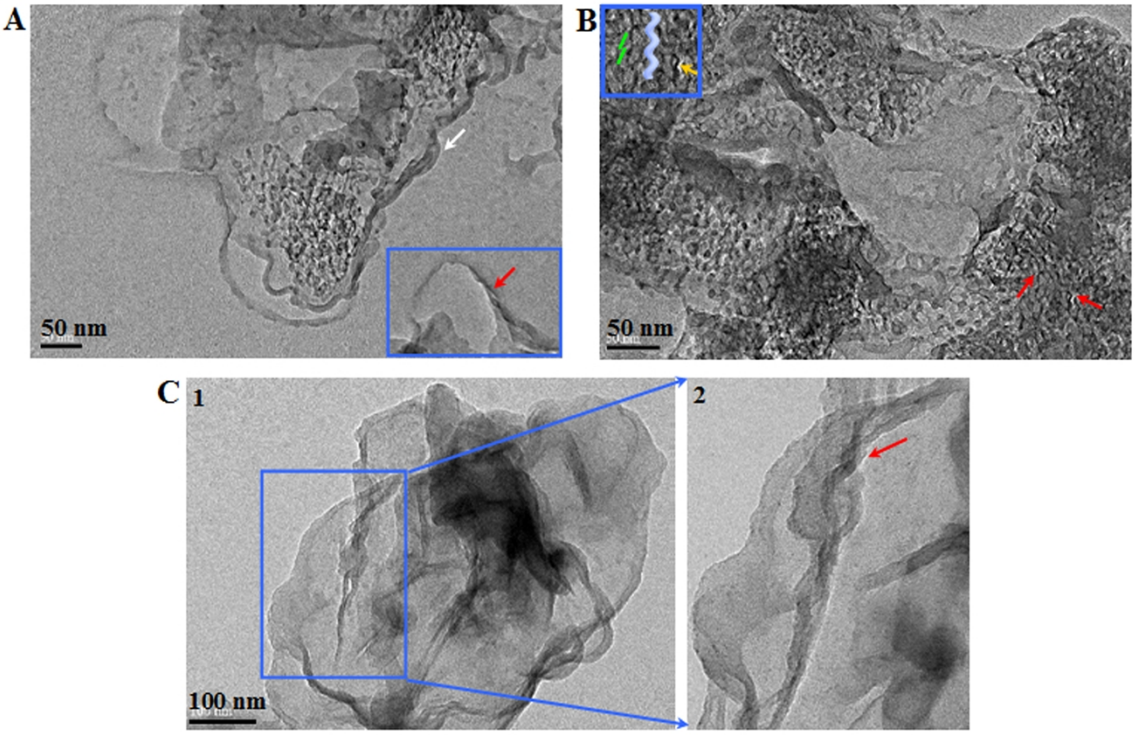

Fig. S3. Dark aggregates and nanofiber structures of PVP-PDP in $CHCl_3$ with a concentration of 1.0×10^{-3} mol·L^{-1}. The size of inserted images in A and B is 125×77 and 58×50 nm^2, respectively, and that of panel 2 in C is 212×265 nm^2.

In Fig. S3A, there exist two kinds of structures. One is the nanofiber with the average width of ~9 nm, which are composed of two intertwined fibrils with the average width of ~4 nm (indicated by the red arrow in the inset of Fig. S3A) and these nanofibers can further intertwist, marked by the white arrow in Fig. S3A. The other is dark aggregates, which are made of many fibrils with spring-like structures. In Fig. S3B together with the insert, one can obviously observe many fibrils in the dark regions, and meanwhile these fibrils with the average width ~4 nm present a typical spring-like structure, consistent with the primary helical structure. Therefore, these dark aggregates greatly correspond to those bright spots in AFM images (Fig. 1A, Fig. S1B and S1C and Fig. S4). Additionally, there are many nanofibers in Fig. S3C. Panel 2 shows a bundle of nanofibers with three nanofibers, of which two nanofibers intertwine into a right-handed helical conformation without further a curve in the opposite helical direction, indicated by the red arrow. Herein, each of nanofibers has an average width of ~9 nm. The results imply that H-IIIs can spontaneously curve into a long coiled coil (spring-like) cable (Fig. 1C and Fig. 2B) in the opposite twisting direction only when their lengths are long enough.

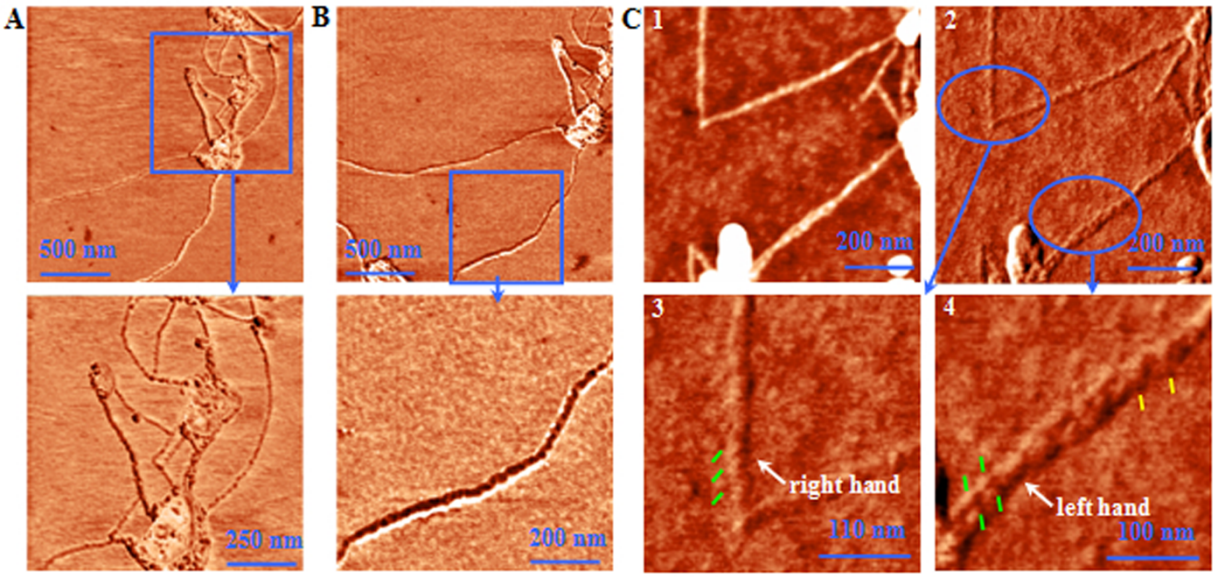

Fig. S4. The single and double-stranded helical structures of PVP-PDP with a concentration of 5.0×10^{-4} mol·L^{-1} on mica at 0 mN/m. In C, panel 2 is the phase image of panel 1, while panels 3 and 4 are zoomed-in images of panel 2.

Fig. S4 shows the single and double-stranded helical structures of PVP-PDP at 0 mN/m. Further analysis of the locally zoomed-in image (panel 4 of Fig. S4C), two intriguing phenomena can be observed: first, a left-handed double helix appears in the upper right corner, of which the helical pitch is about 36 nm, indicated by two yellow oblique stripes; second, two single strands with a left-handed helical structure, marked by two green oblique stripes respectively, create such a left-handed double helix, clearly shown in the lower left corner. In the latter case, the structural characteristics of single strands with the height of ~0.7 nm, the width of *ca*. 5 nm and the helical pitch of about 18 nm are closely identical to that of the helical structure in Fig. 1A. Moreover, after the double-stranded helix is formed, its height, width and helical pitch increase up to ~1.3, 18 and 36 nm, respectively.

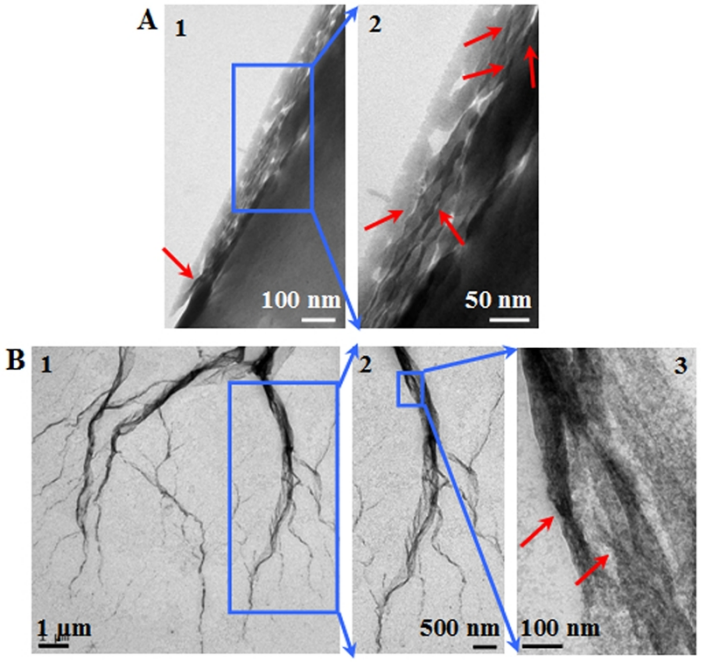

Fig. S5. Advanced aggregates of PVP-PDP in $CHCl_3$ at different concentrations of 1.0×10^{-3} mol·L^{-1} (A) and 5.0×10^{-3} mol·L^{-1} (B).

In Fig. S5A-1 is shown a bundle of nanofibers with a right-handed twisting sense, indicated by the red arrow. Further examination of the bundle in Fig. S5A-2 indicates that this bundle is chiefly composed of many right-handed double helical nanofibers with the width of ~9 nm and the helical pitch of *ca.* 25 nm (denoted by red arrows, typical helices with secondary structure). Additionally, the dark area in the lower right corner of Fig. S5A is attributed to the amorphous film. There are three main stems in Fig. S5B-1. Fig. S5B-2 shows one of the representative stems, as the quaternary structure of helix. It should be noted that this main stem is made up of many bundles of nanofibers via a left-handed twisting way in Fig. S5B-3, which is greatly consistent with the mode in Fig. 2B.

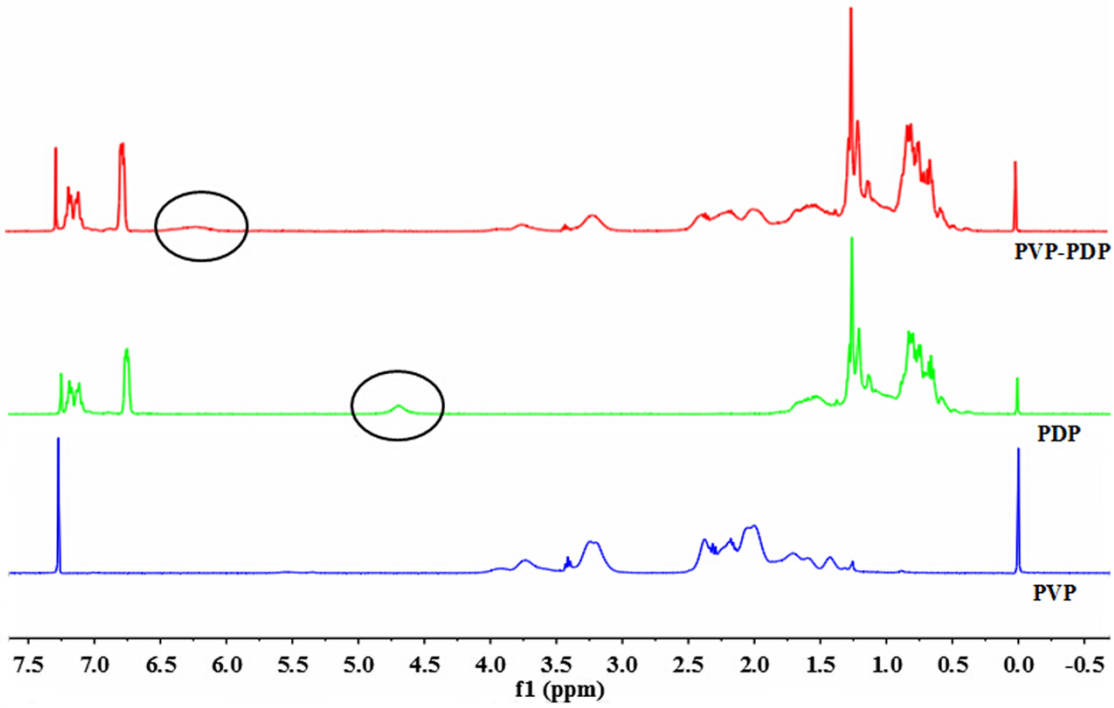

Fig. S6. ^{1}HNMR spectra of PVP, PDP and PVP-PDP in $CDCl_3$ (the concentration in the repeated unit is 5.0 × 10^{-4} mol·L^{-1}).

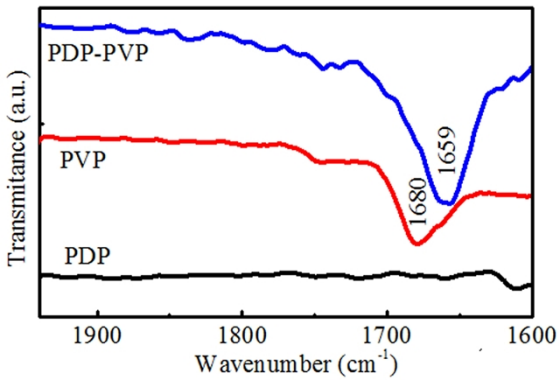

Fig. S7. FT-IR spectra of PVP, PDP and PVP-PDP at 5.0 × 10^{-4} mol·L^{-1}.

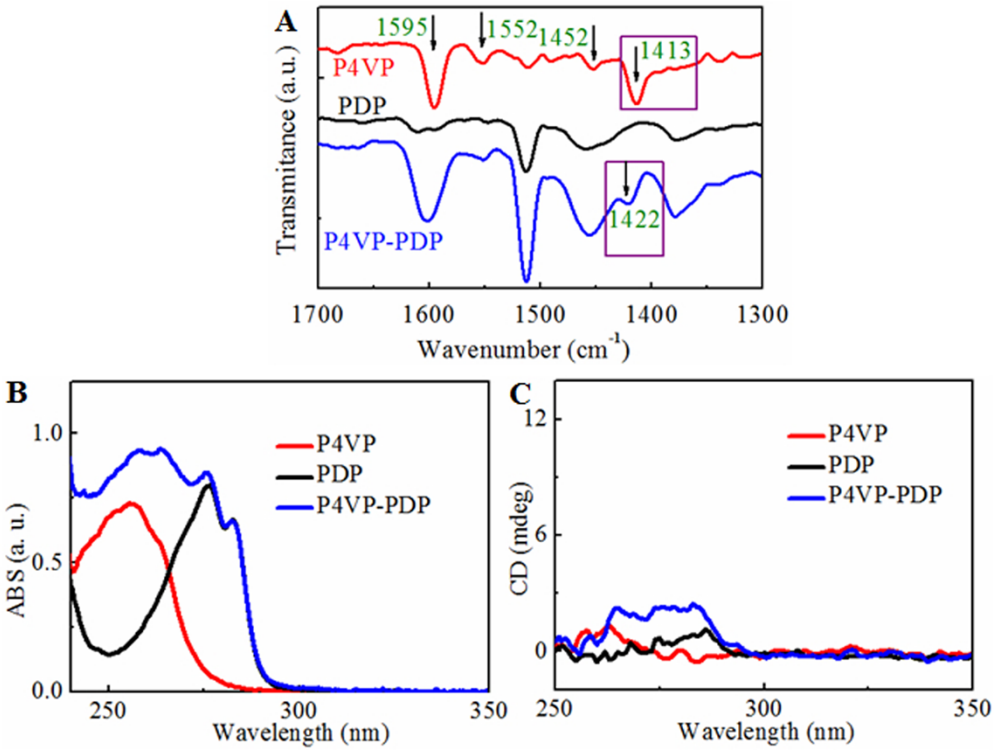

Fig. S8. FT-IR (A), UV-Vis (B) and CD (C) spectra of P4VP, PDP and P4VP-PDP in $CHCl_3$ at 5.0×10^{-4} $mol \cdot L^{-1}$.

In Fig. S9A, the absorption peaks at 1595, 1552, 1452 cm^{-1} can be assigned to the ring vibration of pyridine of P4VP.[1] Note that the aromatic semicircle C=N stretching of pure P4VP appears at 1413 cm^{-1} and shifts to 1422 cm^{-1} (marked by the purple rectangular box) when the sample is 1:1 molar ratio mixture of P4VP and PDP. This result suggests the formation of hydrogen bond at para position between the pyridyl group of P4VP and the phenolic hydroxyl group of PDP.[2] Particularly, CD spectrum of P4VP-PDP shows a negligible CD signal compared to that of PVP-PDP in Fig. 3B. The results indicate that the hydrogen bond at ortho position has a significant effect on the formation of the superhelical structure, rather than at para position.

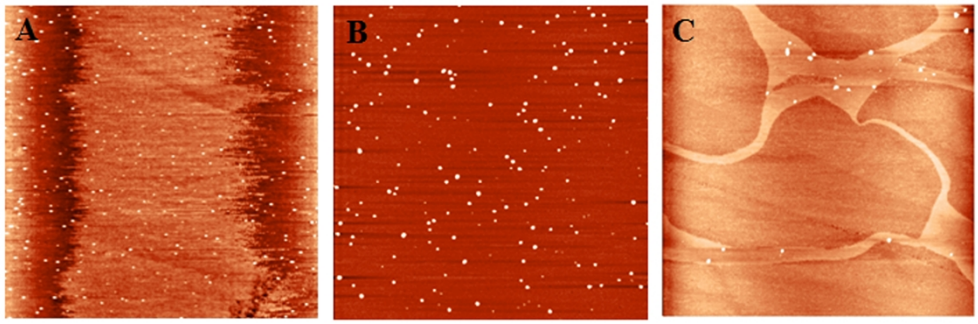

Fig. S9. The AFM images of pure P4VP and P4VP-PDP complex in $CHCl_3$ 5.0×10^{-4} mol·L^{-1}: A), P4VP LB film at 0 mN·m^{-1} (10×10 μm^2); B), P4VP-PDP spin-coating film (10×10 μm^2); C), P4VP-PDP LB film at 0 mN·m^{-1} (30×30 μm^2).

There is no fibril structure whether it is pure P4VP or P4VP-PDP complex. This result is remarkably different from that of PVP-PDP.

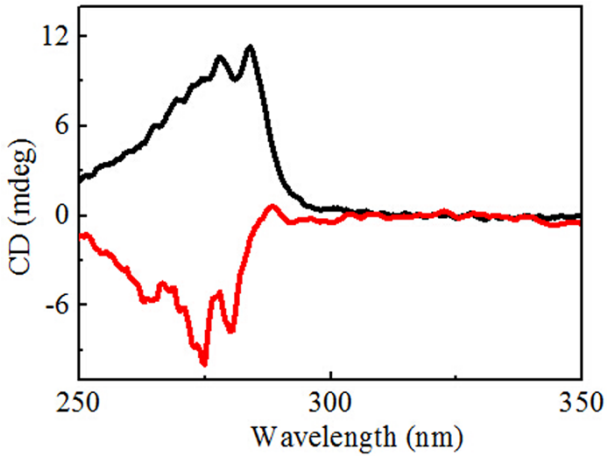

Fig. S10. CD spectra of PVP-PDP in $CHCl_3$ at 5.0×10^{-4} mol·L^{-1}.in different batches.

In Fig. S10, we have fabricated twenty batches of the PVP-PDP in $CHCl_3$ solution and found that all of them showed unsplitted CD signals, in which only two batches exhibited negative CD signals (indicated by the red line) and the others displayed positive signals (denoted by the black line). The results are corresponding to the TEM and AFM images with right-handed or left-handed helical structures.

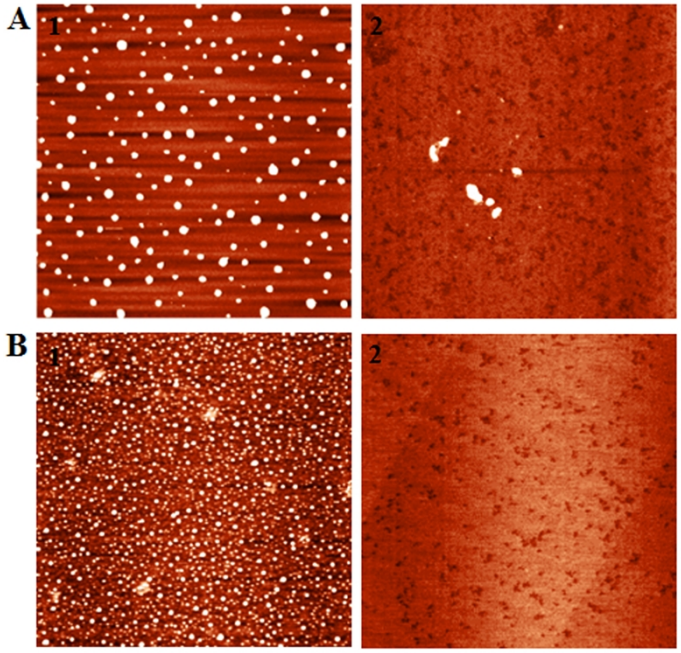

Fig. S11. The morphological comparison between spin-coating (1) and LB (2) films of PVP (A) and PDP (B). Herein, the size of panel 1 and 2 is 10 × 10 and 5 × 5 μm^2, respectively, and LB films were deposited at 2 $mN \cdot m^{-1}$.

REFERENCES

(1) L. Y. Wang, Y. Fu, Z. Q. Wang, Y. G. Fan and X. Zhang, *Langmuir.,* 1999, **15**, 1360-1363.

(2) T. J. Bradley, W. C. E. Schofield, R. P. Garrod and J. P. S. Badyal, *Langmuir*., 2006, **22**, 7552-7555.